



Numerical simulation on a dynamic mixing process in ducts of a rotary pressure exchanger for SWRO

Zhou Yihui*, Ding Xinwei, Ju Maowei, Chang Yuqing

*School of Chemistry, Dalian University of Technology, No. 52 Yinghua Street, Dalian 116012, China
email: Zhou-yihui@163.com*

Received 4 September 2006; Accepted 10 September 2008

ABSTRACT

A rotary pressure exchanger (RPE) is an energy-recovery equipment based on the positive-displacement principle. Since there is no tangible separator in the duct of the rotor, the mixing occurs between the high and low salinity fluids and during the mass and energy transportation. The movement of the mixing zone in the duct works as a liquid piston. The formation and movement of the mixing zone are key factors on the performance of RPE. In this paper, 3.5% NaCl and 1.8% NaCl solutions are selected as the reference fluids. The dynamic mixing process model is set up. The mixing formation, its movement and concentration distribution in the duct are simulated based on the experimental data. The simulation shows that the mixing zone moves reciprocally in the duct and its moving distance remains almost unchanged. After the observation was analyzed, the conclusion for the mixing zone keeping constant moving distance is that the liquid flow rate and the rotor speed substantially cancel each other. This important characteristic of the mixing zone will guarantee the purity of seawater. Although the volumetric efficiency is not very satisfying, the simulation gives theoretical support and future innovation for a rotary pressure exchanger.

Keywords: Rotary pressure exchanger; Mixing; Numerical simulation; Positive displacement; SWRO

1. Introduction

A rotary pressure exchanger is a kind of fluid energy recovery equipment which is based on the positive-displacement principle. Fig. 1 illustrates its operating principle [1]. The key components of RPE include a rotor with several circular ducts, two end covers and one sleeve. At any time during operation, half the ducts are exposed to the high pressure fluid and the other half are exposed to the low pressure fluid. As the rotor turns, one duct is filled with either fresh seawater or a high concentration stream alternatively. When the duct passes the sealing zone, which separates the high pressure fluid from the low pressure fluid, the duct containing the high pressure fluid is separated from the adjacent duct containing the low pressure fluid. The high and low concentration fluids

directly impact each other in the duct and the pressure energy is transferred from the higher fluid to the other. Since there is no tangible separator in the duct, the mixing happens inevitably. The mixing formation and its movement are very important to the performance of the RPE because of its direct effect on the purity of pressurized fluid. If the mixing is out of control, either occupying the whole duct or moving out of the duct, the quality of pressurized fluid will be poor, even though the pressure energy could be recovered without loss. The mixing dynamic formation and its movement play important roles in RPE design and its performance thereafter.

The RPE operating principle is not complex: energy recovery will be achieved as long as the end-face seal is ensured. Moreover, the performance of a dynamic mixing process also depends on the following parameters:

- duct diameter, diameter of ducts circular distribution, rotor diameter, duct length and number of ducts

*Corresponding author.

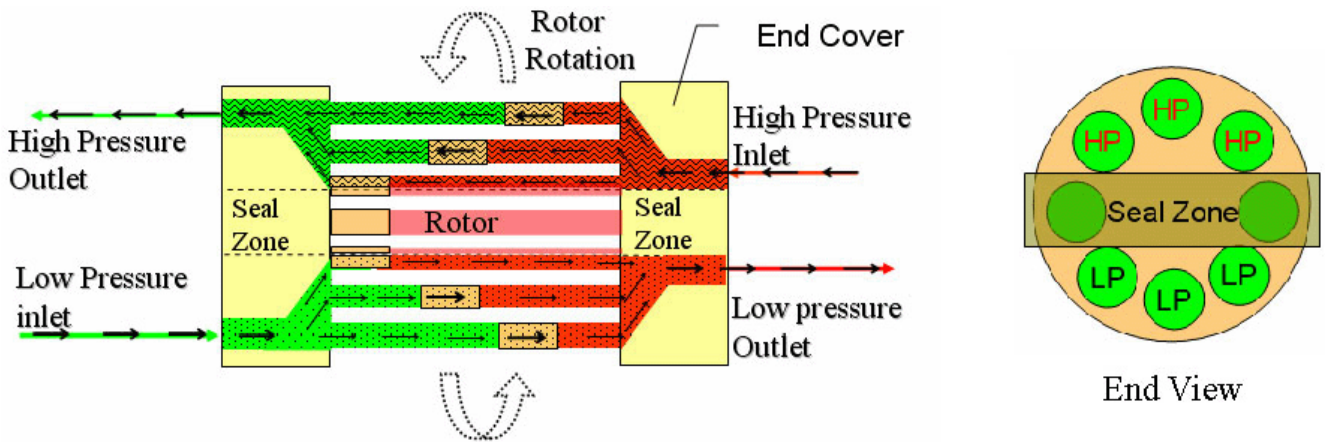


Fig. 1. Structure view of the rotary pressure exchanger.

- process flow rate and rotor speed
- concentration difference between two fluids

The experiments indicate that the above parameters are not independent. These parameters affect the mixing performance as a whole.

2. Theoretical computations on mixing moving distance

For a better quality of pressurized fluid the mixing should meet the following requirements.

- The size of the mixing zone shall be minimized to increase the volumetric efficiency of duct.
- The position/location of the mixing zone shall be unchanged. If the mixing zone expands to the whole duct, the RPE equipment is out of working condition.
- The mixing exchange shall happen inside the duct. If the mixing moves out of the duct, the quality of the pressurized fluid will be poor.

To meet the above requirements, an equal in length of the mixing zone reciprocating in one duct is required when the duct is exposed to low-pressure and high-pressure respectively. The closer the moving distance vs. the full length of the duct, the higher the volumetric efficiency of rotor duct will be.

The mixing zone can be treated as a membrane whose thickness is neglected. The flow-in length of the duct can be computer-stimulated, based on the experimental data of the flow rate and rotor speed shown in Fig. 2. The experimental equipment is made of F4 and an eight-duct rotor.

The actual moving distance of the mixing zone

$$l_m = \frac{Q_r}{A} = \frac{vS}{A} \tag{1}$$

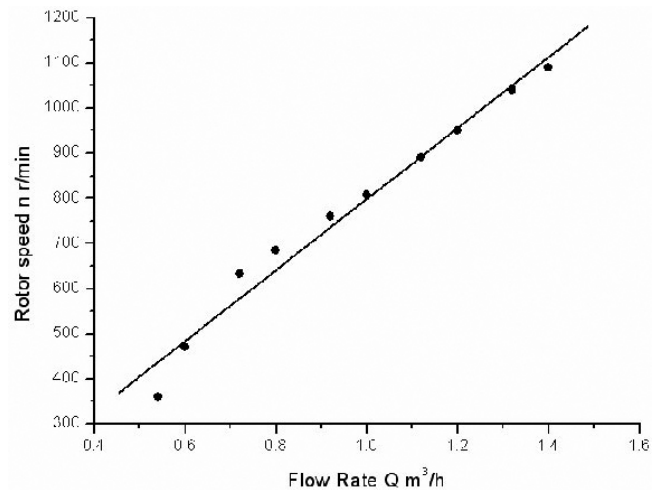


Fig. 2. Relationship between flow rate and rotor speed.

The mixing zone moving velocity is

$$v_m = \frac{l_m}{T} \tag{2}$$

In each equation, *S* represents the integral area of duct switching in and out with the inflow pipe, which is the function of the rotor speed and the geometry of the ducts distribution (Fig. 3).

$$S = \int_0^T \omega f(dt) \tag{3}$$

The relationship between the process fluid flow rate, rotor speed, mixing zone velocity and its moving distance is illustrated in Fig. 4 in arbitrary units. The mixing velocity increases as the flow rate increases; however, the

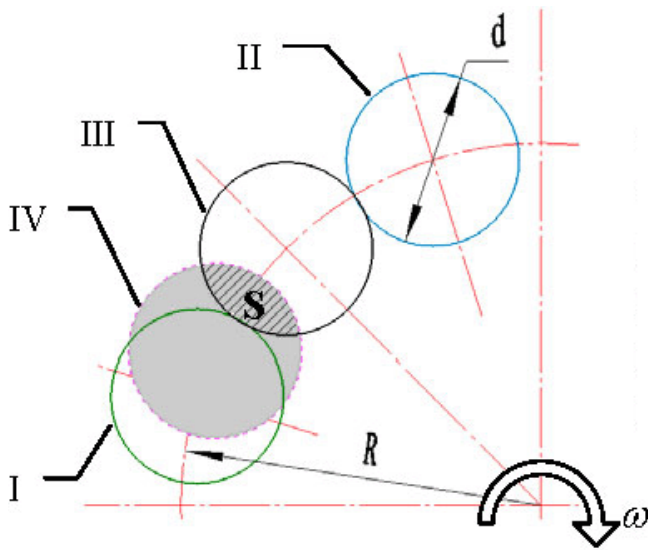


Fig. 3. Computation of S. I, duct position when switching in the inflow pipe; II, duct position when switching out of the inflow pipe; III, inflow pipe position; IV, duct position during rotation.

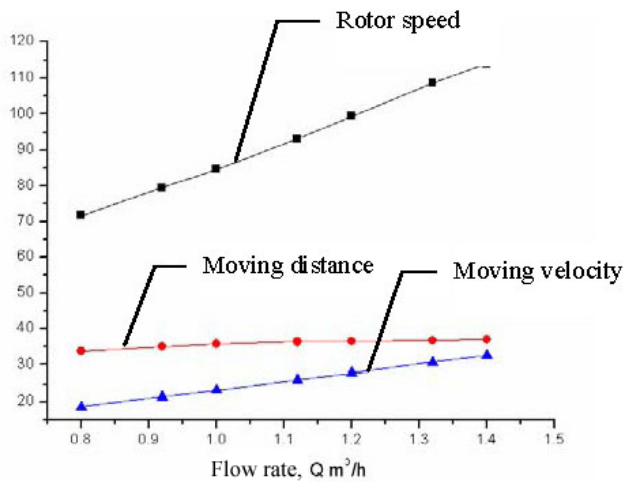


Fig. 4. Rotor dynamic computation result.

rotor also speeds up to give the mixing less time to move in the duct. When the rotor speed is higher than 1000 r/min, the mixing length will keep almost constant (within 4 mm). At this point, the RPE will be able to be adjusted to the fluid fluctuation with an intangible liquid plug. The slope of the black curve in Fig. 5, which characterizes the responsiveness of the rotor to flow, is fixed by the design of RPE. The variation of the mixing zone moving velocity and the rotor speed with flow substantially cancel such that the distance the high–low pressure interface moved in the rotor duct, which varies little over the RPE operating range. Accordingly, the performance degree of mixing between the streams varies little with the process flow rate [1].

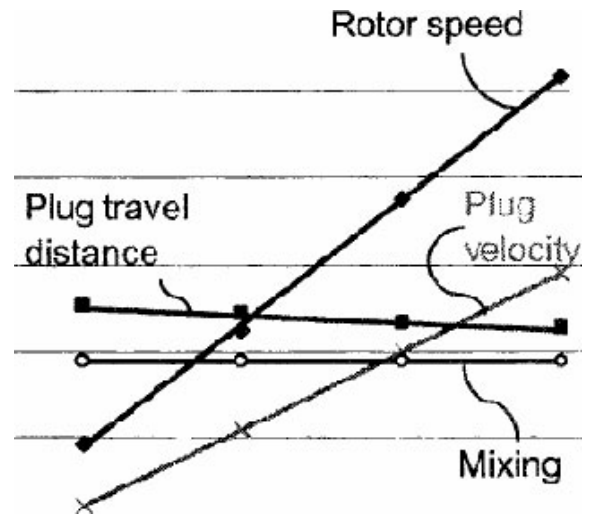


Fig. 5. Results from Stover [1].

3. Mixing process simulation

3.1. Geometry model

Fig. 6 illustrates the geometry model of the simulation. 3.5% and 1.8% NaCl solutes are used for the simulation and treated as incompressible and inviscid fluids. The fluid storage intends to prevent any of pressure upset and flow rate variation. The initial conditions are given in Table 1.

3.2. Physical model [2,3]

The control equations are:

- Mass conservation

$$\frac{\partial \rho}{\partial t} + \text{div}(\rho \mathbf{u}) = 0$$

for incompressible fluid

$$\frac{\partial u}{\partial x} + \frac{\partial v}{\partial y} + \frac{\partial w}{\partial z} = 0 \quad (4)$$

- Momentum conservation was to Euler

$$\rho \frac{D\mathbf{u}}{Dt} = \rho \mathbf{F}_b - \text{grad } p \quad (5)$$

- Energy conservation

$$\frac{\partial(\rho T)}{\partial t} + \text{div}(\rho \mathbf{u} T) = \text{div} \left(\frac{k}{C_p} \text{grad } T \right) + S_T \quad (6)$$

which could be neglected because the energy transferring process is adiabatic for a short time of touch.

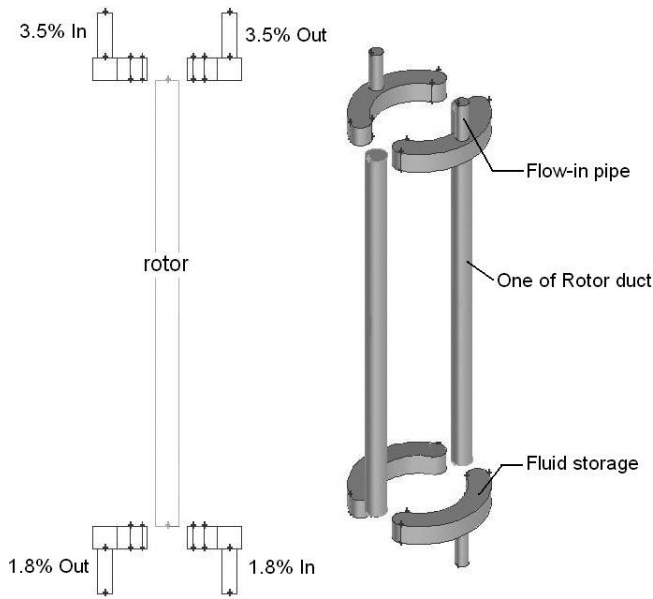


Fig. 6. Geometry model for simulation.

- Species transport equation

$$\frac{\partial(\rho c_s)}{\partial t} + \text{div}(\rho \mathbf{u} c_s) = \text{div}[D_s \text{grad}(\rho c_s)] + S_s \quad (7)$$

- Turbulence model: standard k - ϵ model. The turbulence kinetic energy, k , and its rate of dissipation, ϵ , are obtained from the following transport equations:

$$\frac{\partial(\rho k)}{\partial t} + \frac{\partial(\rho k u_i)}{\partial x_i} = \frac{\partial}{\partial x_j} \left[\left(\mu + \frac{\mu_t}{\sigma_k} \right) \frac{\partial k}{\partial x_j} \right] + G_k - \rho \epsilon \quad (8)$$

$$\frac{\partial(\rho k)}{\partial t} + \frac{\partial(\rho k u_i)}{\partial x_i} = \frac{\partial}{\partial x_j} \left[\left(\mu + \frac{\mu_t}{\sigma_\epsilon} \right) \frac{\partial \epsilon}{\partial x_j} \right] + G_{1\epsilon} \frac{\epsilon}{k} (G_k + G_{3\epsilon}) - C_{2\epsilon} \rho \frac{\epsilon^2}{k} \quad (9)$$

The computation is carried with FLUENT6.2 after the parameters in control equations are set up in the software.

Table 1
Initial conditions for simulation

Diameter of duct, d /mm	12
Length of duct, L /mm	300
Circular angle of fluid storage, θ	120
Rotor speed, n / r/min	1200

4. Simulation results and discussion

4.1. Computation time for a steady field result

At the initial conditions the field is filled with 1.8% fluid. The energy transportation and mixing process have not reached equilibrium till the steady mixing is formed. After the steady mixing is formed on the basis of inspecting the species concentration on the low pressure outlet face, the computation is completed. Table 2 shows the computation conditions. Fig. 7 illustrates the appropriate time being 3–3.5 s.

4.2. Pressure effect on the mixing computation

During operation the ducts rotate between high and low pressure area alternatively with pressure difference between inlet and outlet of ducts being 0.5 MPa. The effect of the pressure difference on the mixing formation has been researched to save computation time. Fig. 8(a) shows the mixing in one duct when it is in high pressure area, and Fig. 8(b) shows the duct in low pressure area, with the right one being the result of computation with pressure difference in both situations.

It has been observed that the 0.5 MPa pressure difference has no obvious effect on the mixing formation. Therefore, the pressure difference between inlet and outlet of duct is negligible in the simulation.

4.3. Mixing formation in the duct

Fig. 9 illustrates the different positions of one duct during one rotation period. The rotation starts from 1 and high pressure the 3.5% NaCl flows into the duct when the duct is in position 1 and 2. At the same time the 1.8% NaCl is pressurized. The mixing zone is formed in the duct and after a seal area, position 3 and 4. The 1.8% NaCl is closed to be pushed out of the duct and the flow-in length of high pressure fluid goes to its maximum. Then, the 1.8% NaCl enters the duct in positions 5 and 6, and after another seal area, positions 7 and 8, the 3.5% NaCl is closed to be pushed out of the duct and the flow-in length of low pressure fluid reaches its maximum. After these, the duct returns to position 1, and the rotation and pressure exchanger process recycle again. It is clearly seen that the

Table 2
Computation conditions for steady mixing formation

Rotor speed, r/min	Flow rate, m ³ /h	Flow velocity, m/s	Species concentration, %	Steady time, S
600	1.024	1.415	3.5–1.8	3
1200	1.405	1.941	3.5–1.8	3

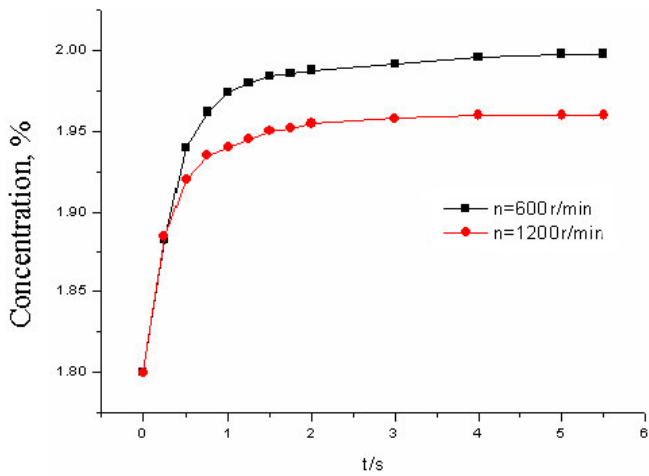


Fig. 7. Concentration on outlet face.

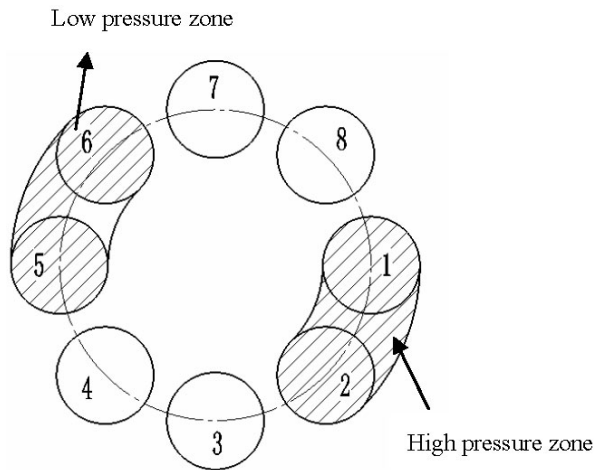


Fig. 9. Position of ducts.

mixing is formed and moves reciprocally in the duct. The stable mixing zone works as a liquid piston to separate two fluids and the purity of pressurized fluid is guaranteed.

Because the duct is filled with a liquid plug and flow-in fluid, the flow-in length is one of the key factors on the rotor performance. The longer the flow-in length is, the shorter the mixing zone will be, and the higher the volumetric efficiency will be as well.

4.4. Parameters of duct effect on flow-in length

Fig. 11 illustrates the effect of rotor parameters on the flow-in length. Generally speaking, the rotor parameters play less important roles on the flow-in length because of few variations of maximum flow-in length. With a stable flow rate, the maximum flow-in length decreases as the diameter of the duct increases. The maximum flow-in length occurs at optimization of the duct quantity and

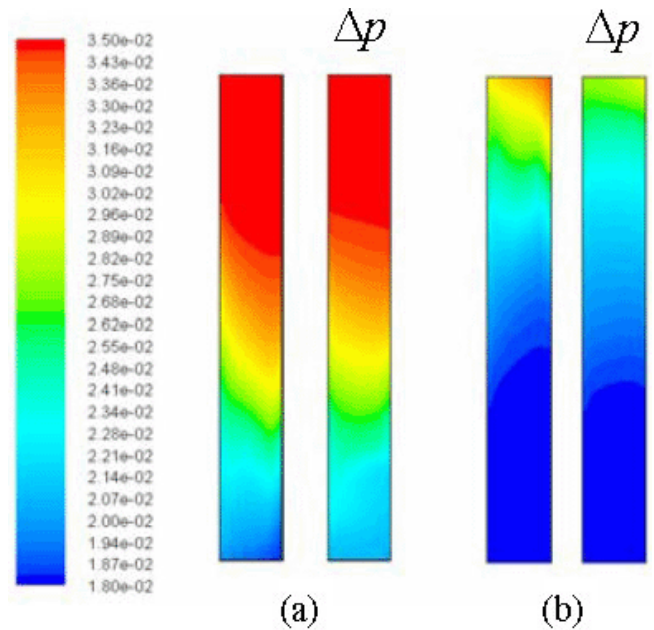


Fig. 8. Mixing formation with pressure effect.

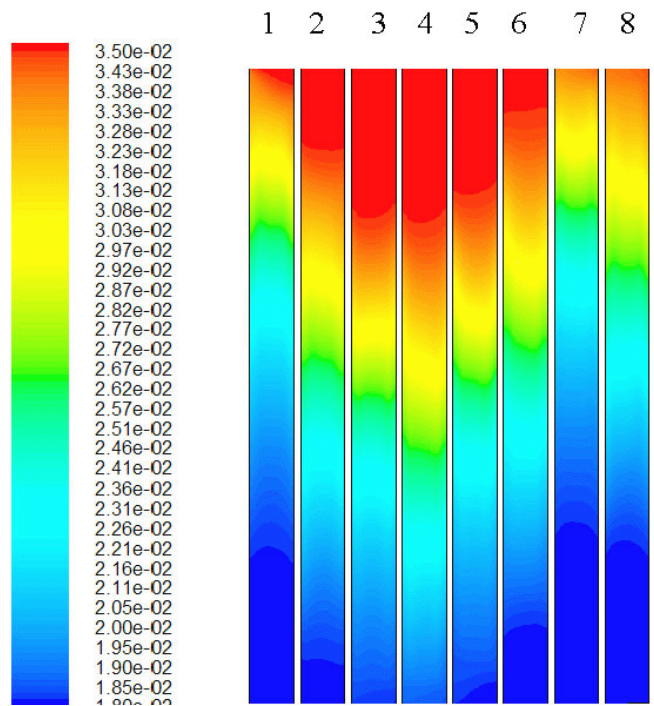


Fig. 10. Concentration distribution in duct during rotation.

length of the duct. When the number of the ducts is greater than 12 and the length of the duct length is longer than 200 mm, the efficiency of flow-in length decreases.

4.5. Working conditions effect on flow-in length

Fig. 12 illustrates the effect of different working conditions on the flow-in length. The working conditions

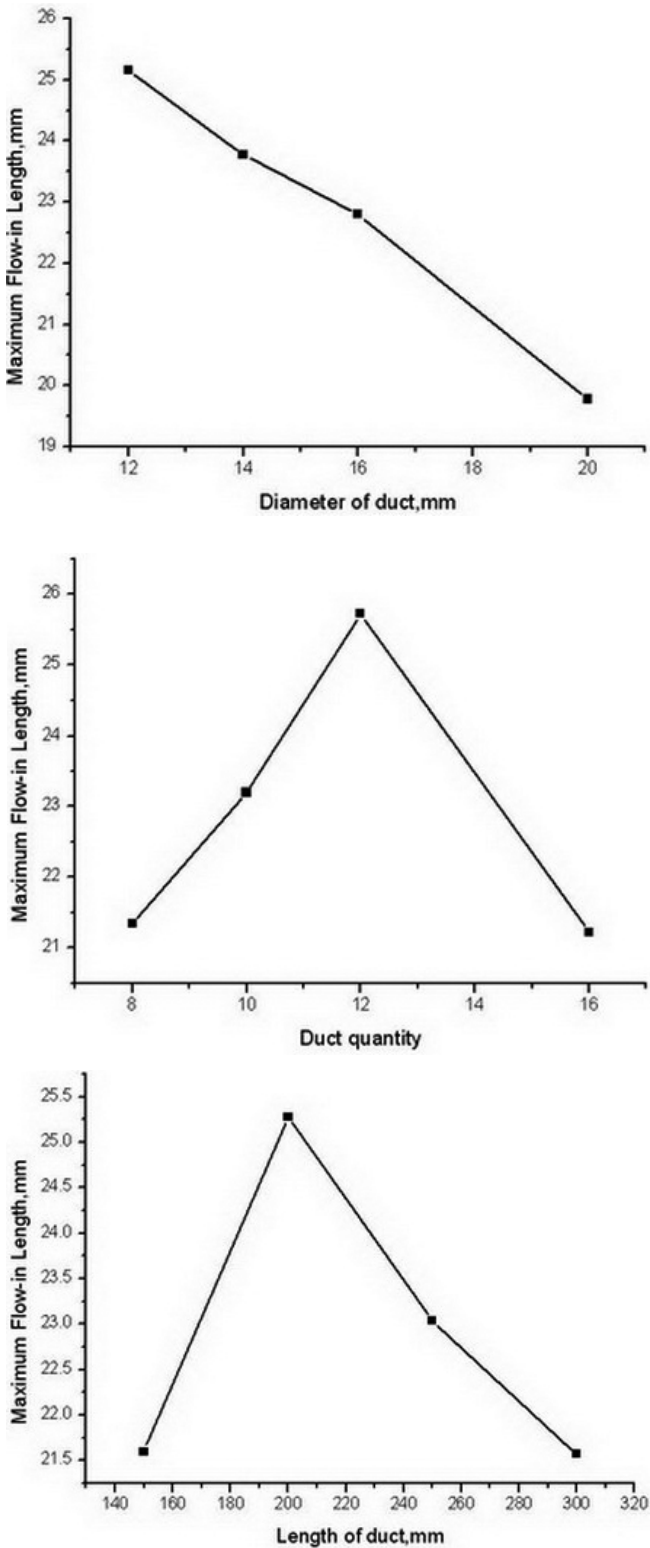


Fig. 11. Relationship of rotor parameters and maximum flow-in length.

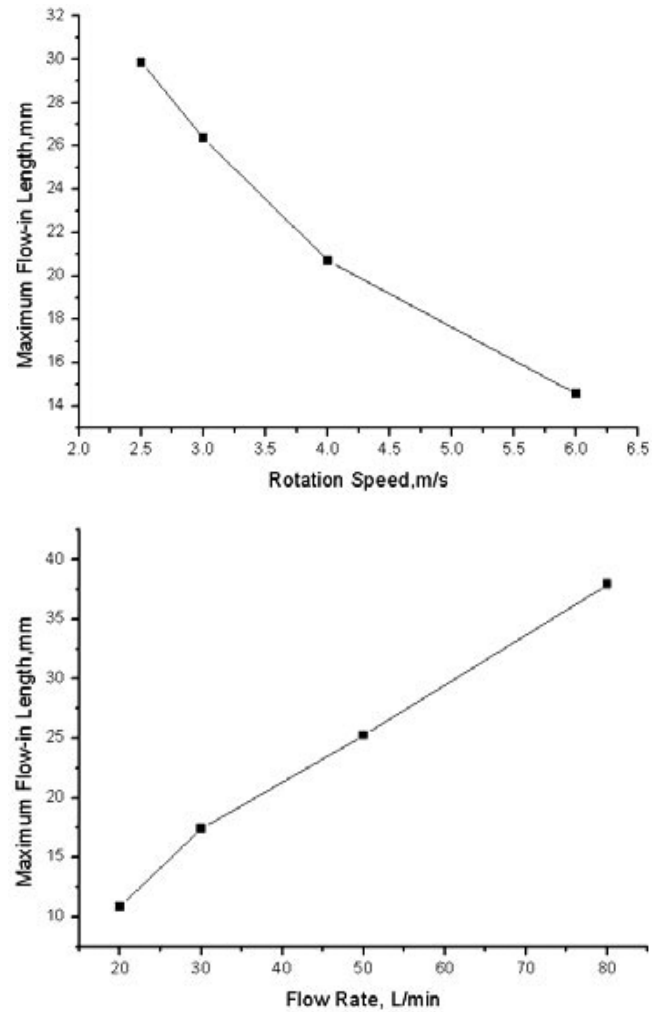


Fig. 12. Relationship of rotor parameters and maximum flow-in length.

have more effects on the maximum flow-in length than the rotor parameters. The flow-in length decreases as the rotation speed increases simply because the fluid entering the duct decreases. The increasing flow rate has a positive effect on the flow-in length.

5. Conclusions

The dynamic mixing model is set up according to a fluid-driven rotary pressure exchanger. The dynamic mixing process is simulated to get the steady mixing formation time, the mixing formation process and their effective parameters. Simulation results show that pressure difference has no effect on the mixing formation. During rotation the mixing zone reciprocally moves in the duct. Both the rotor parameters and the working conditions have more effects on the maximum flow-in length which could affect the rotor performance. The rotor speed

and the process flow rate cancel each other, therefore the moving distance of the mixing zone keeps constant when working conditions have no changes.

6. Symbols

- A — Cross area of the duct, m^2
 l_m — Moving distance of the mixing zone in the duct, m
 Q_V — Flow rate entering the duct, L/min
 S — Interarea of the duct in the high or low pressure system, m^2
 v — Process flow velocity, m/s

- v_m — Moving velocity of the mixing zone in the duct, m/s
 T — Rotation period from switching in to out of the pressure system, s
 ω — Rotation angular speed of the rotor, rad/s

References

- [1] R.L. Stover, Development of a fourth generation energy recovery device. *Desalination*, 165 (2004) 313–321.
- [2] F. Wang, *Computational Fluid Dynamics Analysis*, Tsinghua Press, Beijing, 2004.
- [3] Z. Han and J. Wang, *Fluent Engineering Application*, Beijing University of Technology Press, Beijing, 2004.